Springer

KSME

Journal of Mechanical Science and Technology 28 (11) (2014) 4737~4744

www.springerlink.com/content/1738-494x
DOI 10.1007/s12206-014-1040-3

The influence of alumina on mechanical and tribological characteristics of graphite particle reinforced hybrid Al-MMC †

A. Arun Premnath[1,*], T. Alwarsamy[2], T. Rajmohan[1] and R. Prabhu[1]

[1]*Sri Chandrasekharendra Saraswathi Viswa Maha Vidyalaya University, Enathur, Kanchipuram - 631561, Tamilnadu, India*
[2]*Liaison officer, Directorate of Technical Education Chennai, India*

(Manuscript Received August 4, 2013; Revised June 25, 2014; Accepted July 17, 2014)

Abstract

We consider the influence of alumina (Al_2O_3) particles on mechanical and tribological properties of aluminum hybrid metal matrix composites (MMC). Various weight fraction of Al_2O_3 (5, 10 and 15%) and constant weight fraction of graphite (5%) were used to fabricate composites by stir casting method. The effect of Al_2O_3 content on hardness, density and specific wear rate is evaluated. A wear test was performed using central composite design matrix on a pin-on disc apparatus at room temperature for constant sliding distance of 1000 m. The sliding speed, load and weight fraction of Al_2O_3 were the process variables. The results show that the hardness and density increase with increase in Al_2O_3 content. From the analysis of variance (ANOVA), load is the dominant factor that affects the specific wear rate of hybrid composites followed by speed and weight fraction of Al_2O_3. Based on desirability approach, the improvement in the wear resistance of the composites became more prominent at high speed, high load and high weight fraction of Al_2O_3. The worn surface of the pin was examined using scanning electron microscope (SEM) which indicates that the wear mechanism of composites is mostly abrasive wear followed by oxide wear.

Keywords: Density; Hardness; Hybrid composites; Scanning electron microscope; Specific wear rate

1. Introduction

Aluminum reinforced with hard ceramic particles such as Al_2O_3, SiC, BiO_2 improves the strength to weight ratio, mechanical properties, wear resistance etc. that makes it suitable for tribological applications. Several fabrication techniques are available, such as stir casting, spray deposition, die casting and powder metallurgy for producing a near net shaped MMC component with good surface finish. Stir casting is commonly used because it is economical. It is noted that, particle volume fraction, particle size and matrix properties are the factors that affect the mechanical and tribological properties of composites. Aluminum (Al) 6061 reinforced with Al_2O_3 is used in automotive applications such as piston rings, connecting rods, and engine blocks. Since these components are subjected to enormous amount of wear, wear resistance is more essential. The implementation of hard ceramic particles into the matrix alloys improves their mechanical and tribological behavior. The addition of graphite (Gr) particle acts as solid lubricant, thereby reducing the co-efficient of friction and increasing the wear resistance during dry sliding condition. The main requirements of automobile components such as engine pistons, cylinder liners, and brakes are superior mechanical properties coupled with better wear resistance. This can be achieved by Hybrid MMC which has more than one reinforcement, namely hard and soft particles [1].

In the past two decades, considerable works have been reported on mechanical and tribological properties of composites. Bushan et al. [2] fabricated Al 7075-SiC composites with various weight fraction and size using stir casting method. Muthu Kumar et al. [3] used infiltration process to prepare Mg/SiCp and AZ91/SiCp to study the wear properties. Prashanth et al. [4] fabricated Al glass fiber MMC using powder metallurgy method and depicted the influence of glass fiber on mechanical properties of composites. Reddy et al. [5] used microwave processing method to fabricate copper-TiC-graphite hybrid metal matrix composites and investigated the effects of physical and mechanical properties. Wenlin et al. [6] conducted experiments to study the effect of sliding speed on friction and wear performance of a copper-graphite composite and concluded that the coefficient of friction and wear rate of copper-graphite composites are largely dependent on sliding speed. Rajeev et al. [7] studied the influence of wear and friction with respect to applied load, sliding distance, reciprocating velocity, counter surface temperature and silicon content in Al/SiC composites. Sai et al. [8] studied the dry sliding

*Corresponding author. Tel.: +91 9994346132, Fax.: +91 44 27264285
E-mail address: arun_premnath@kanchiuniv.ac.in
† Recommended by Associate Editor In-Ha Sung

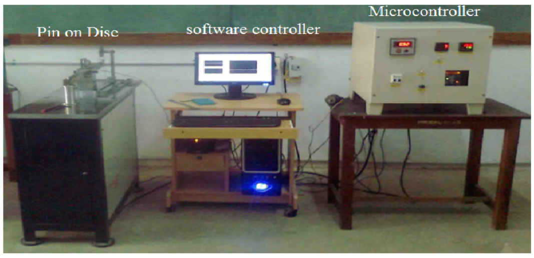

Fig. 1. Pin on disc set-up.

wear behavior of copper fly ash composites using a pin on disc machine. From the results they observed that hardness and density increased for copper coated fly ash particles than the uncoated particles. Akgun et al. [9] studied the dry and water lubricated wear behavior of Al/SiC composites using ball on disc method. Goo and Kim [10] studied the mechanical and tribological behavior of A356/SiC and A390/SiC composites of 30 μm and 60 μm SiC particles with 20%volume fraction. From the result they concluded that the tensile strength of A356 alloy is higher than that of A356/SiCp which is mainly due to formation of voids during fabrication. They also reported that A390/SiCp composites are more wear-resistant than A356/SiCp composite. Park et al. [11] analyzed the wear characteristics of Al-based composite with Ni preform as reinforcement using a Ball on Disc method. They found that wear resistance properties of Ni/AC8A composites are better than matrix AC8A. Liu et al. [12] studied the tribological properties of Ni-based composites reinforced with Ag_2MoO_4 powder in a pin-on-disc tribometer. From the wear test result they found that Ni-based composites containing graphite and silver molybdate lubricants exhibited superior tribological properties at ambient and high temperatures.

From the above literature, it is concluded that most of the researches are related to wear of either on abrasive particles or on soft particles as reinforcements to MMC'S. But very marginal work is found on both reinforced hybrid composites. Therefore, our aim is to understand the effect of Al_2O_3 on mechanical and tribological characteristics of graphite reinforced hybrid composites.

2. Experimental procedure

2.1 Fabrication of composites

Al 6061 was used as the matrix material and its composition is shown in Table 1. Al_2O_3 of size 45 micron and graphite of size 60 micron were used as reinforcements. The Al_2O_3 content varied from (5, 10 & 15%) while graphite (5%) content remained fixed, to study the effect of Al_2O_3 in graphite reinforced aluminum Hybrid MMC. The composites were fabricated to cylindrical shapes of 100 mm in diameter and 300 mm in length using stir casting method. The following steps are used to prepare Hybrid MMC. Al 6061 is melted in a furnace around 800°C and preheated Al_2O_3 particle (500°C) is slowly added with good stirring with a graphite stirrer at 600 rpm. The time of mixing as well as mixing rates are adjusted according to the amount of the reinforcement particles. Ensuring the complete mixing of Al_2O_3, the Al/Al_2O_3 mixture is continued to stir at constant speed for 15 minutes, which enables proper mixing of Al_2O_3. Then pre-heated graphite is added to the mixture and is continuously stirred at 400 rpm for 30 minutes. Care should be taken to avoid inhomogeneous mixing of the mixture, as particle agglomeration and sedimentation during the melt may occur. The Al/Al_2O_3/ Gr mixture then is poured into cast iron moulds. The surfaces of moulds are cleaned using emery to eliminate the exposure of molten composite to pockets of oxidized surface on the cast iron moulds. Then they are pre-heated for about 20 minutes by keeping them over the furnace. The composite mixture is allowed to solidify for about 15 minutes. Thus three different weight fraction of Al_2O_3 based Hybrid MMC are fabricated.

Table 1. Chemical composition of 6061 Aluminum alloy.

Element	Si	Cu	Mg	Mn	Fe	Zn	Sn	Ti	Pb	Al
Weight (%)	0.80	0.35	0.8	0.02	0.01	0.008	0.01	0.01	0.02	97.9

2.2 Testing of composites

Hardness tests are performed on composites to know the effect of Al_2O_3 particles in the matrix materials. The hardness of a material determines the strength of materials. The polished composite specimens are tested for their hardness, using Rockwell hardness testing machine with diamond indenter for 100 kgf load. The load is applied for 30 secs. The Rockwell B-scale hardness test is commonly applied to quantify the mechanical strength of a wide range of particle reinforced MMC and Al alloys [13]. Five sets of readings were taken on the specimen on various places to assess the reproducibility and an average value was calculated. The density of the composites can be calculated theoretically by rule of mixture by using the formula

$$\rho_{th} = \rho_m V_m + \rho_{r1} V_{r1} + \rho_{r2} V_{r2}, \quad (1)$$

where V_m and V_{r1} and V_{r2} represent the volume fraction of matrix and reinforcements, respectively. The density of the aluminum, Al_2O_3 and graphite is 2.70, 3.95 and 2.22 g/cm^3, respectively. The density can be experimentally measured by Archimedean method by weighing the cut portion of cast composites in air and in water. The obtained composite specimen is machined to a pin of 2.5 mm in diameter and 10 mm in length. The pin is rubbed against a disc of 55 mm in diameter made of EN 45 steel of 65 HRC. A wear test is performed on pin-on disc machine (make - Ducom, Bangalore) as shown in Fig. 1 as per ASTM G99-95 standard at room temperature. The specimen initial weight is calculated by using an

Table 2. Process variables used.

Sl.No	Notation	Unit	Limits		
			-1	0	1
Speed	s	m/s	0.8	1.6	2.4
Load	f	N	10	20	30
Weight fraction Al_2O_3	w	%	5	10	15

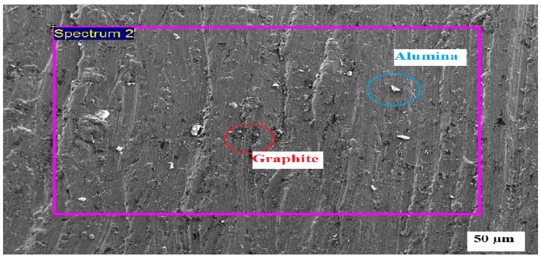

Fig. 2. SEM images showing even distribution for $Al/5Al_2O_3/5Gr$.

electronic weighing balance having an accuracy of 0.0001 g. During sliding the pin is pressed against steel disc for a fixed sliding distance of 1000 m. After the test, the specimen is cleaned with acetone to remove the wear debris and the final weight of the specimen is calculated. The difference in the weight of the specimen before and after the test gives the wear loss. Using the corresponding density values the wear loss is converted to volume loss. From the volume loss the specific wear rate is calculated using the formula

$$\textit{Specific Wear rate } (R) = \frac{W}{F \times D} \quad (mm^3/Nm), \qquad (2)$$

where W (mm^3) is the volume loss, F (N) is the applied load and D (m) is the sliding distance.

2.3 Response surface methodology

The response surface methodology (RSM) technique is a dynamic and foremost important tool, wherein the relationship between responses of a process with its input decision variables is mapped to achieve the objective of maximization or minimization of the response properties [14]. The objectives of quality improvement, including reduction of variability, improved process and product performance, can often be accomplished directly using RSM. In the RSM, the quantitative form of relationship between the desired response and independent input variables, is represented as follows

$$Y = f(s, f, w), \qquad (3)$$

where Y is the desired response and f is the response function and s, f and w represent speed, load and weight fraction of Al_2O_3, respectively. To study the effect of the process parameters a second-order polynomial response surface can be fitted into the following equation:

Table 3. Design matrix and corresponding response.

Sl. No	Run	Coded variables			Actual variables			Specific wear rate (mm^3/Nm)
		s	f	w	s	f	w	
1	6	-1	-1	-1	0.8	10	5	8.03E-07
2	19	+1	-1	-1	2.4	10	5	4.74E-07
3	15	-1	+1	-1	0.8	30	5	3.64E-07
4	2	1	+1	-1	2.4	30	5	1.92E-07
5	18	-1	-1	+1	0.8	10	15	6.29E-07
6	4	+1	-1	+1	2.4	10	15	1.50E-07
7	1	-1	+1	+1	0.8	30	15	3.03E-07
8	9	+1	+1	+1	2.4	30	15	1.15E-07
9	20	-1	0	0	0.8	20	10	4.92E-07
10	7	+1	0	0	2.4	20	10	2.30E-07
11	5	0	-1	0	1.6	10	10	5.00E-07
12	16	0	+1	0	1.6	30	10	2.44E-07
13	10	0	0	-1	1.6	20	5	3.80E-07
14	14	0	0	+1	1.6	20	15	2.44E-07
15	8	0	0	0	1.6	20	10	3.03E-07
16	12	0	0	0	1.6	20	10	3.20E-07
17	13	0	0	0	1.6	20	10	3.20E-07
18	11	0	0	0	1.6	20	10	3.20E-07
19	17	0	0	0	1.6	20	10	3.20E-07
20	3	0	0	0	1.6	20	10	3.20E-07

$$Y = \beta_0 + \sum_{i=1}^{k}\beta_i X_i + \sum_{i=1}^{k}\beta_i X_i^2 + \sum_i \sum_j \beta_{ij} X_i Y_j + \xi , \qquad (4)$$

where, 'Y' is the corresponding response, and x_i is the value of the i^{th} process parameter. β are the regression co-efficient, and ξ is the residual measure, resulting from an experimental error in the observations. This quadratic model works quite well over the entire factor space.

The test is designed based on a RSM using central composite design (CCD) technique. It is a factorial or fractional factorial design with center points and star points. The test is carried out for three- factor-three levels CCD with full replication. The process variables used are shown in Table 2. Design matrix and corresponding response are shown in Table 3. Using ANOVA, the significance of input parameters is evaluated. Design-Expert 10 software is used to establish the design matrix, to analyze the experimental data and to fit the experimental data to a second-order polynomial. Sequential F test, lack-of-fit test, and other adequacy measures are used to check the model's performance.

3. Results and discussion

3.1 Microstructure

The microstructure of the cast hybrid composites is shown

Table 4. ANOVA results.

Source	Sum of squares	df	Mean square	F value	p-value prob > F	
Model	5.03E-13	7	7.19E-14	344.3912	< 0.0001	Significant
s-Speed (m/s)	1.78E-13	1	1.78E-13	853.2346	< 0.0001	
f-Load (N)	2.31E-13	1	2.31E-13	1107.573	< 0.0001	
w-wt of alumina (%)	4.58E-14	1	4.58E-14	219.3916	< 0.0001	
sf	1.57E-14	1	1.57E-14	75.3864	< 0.0001	
fw	8.9E-15	1	8.9E-15	42.63617	< 0.0001	
s^2	9.46E-15	1	9.46E-15	45.29181	< 0.0001	
f^2	1.33E-15	1	1.33E-15	6.356964	0.0268	
Residual	2.51E-15	12	2.09E-16			
Lack of fit	2.27E-15	7	3.24E-16	6.71874	0.0261	Non significant
Pure error	2.41E-16	5	4.82E-17			
Cor total	5.06E-13	19				
R^2						0.99
Adj R^2						0.98

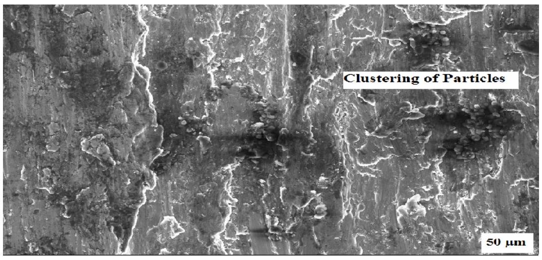

Fig. 3. SEM images showing clustering particles for Al/15Al_2O_3/5Gr.

in the Figs. 2 and 3. From Fig. 2, the Gr and Al_2O_3 particles are evenly spread throughout the specimen. The uniform distribution of reinforcement and good interfacial bonding between the reinforcements and the matrix improves the mechanical properties of the composites. From Fig. 3, it is inferred that the particles get clustered at some places, which is usually seen in higher weight fraction of the reinforcement. Fig. 3 shows some porosity, which is always associated with stir casting method as air entrapped into the molten metal. The EDAX (energy dispersive X-ray analysis) shown in the Fig. 4 reveals the composition of the cast specimens. The specimen consists only of major peaks of aluminum and graphite in the cast specimen as expected and no reaction products are found.

3.2 Hardness and density

The density of the composites obtained from rule of mixture and Archimedean method is shown in Fig. 5. It is clear that both the values are closer to each other. The density obtained from rule of mixture is greater than the Archimedean method; the lower density values by Archimedean method are due to the increased porosity [15]. Also, the density of composites

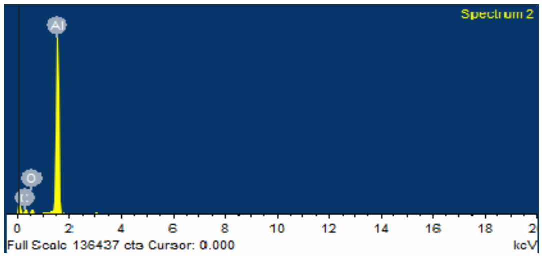

Fig. 4. EDAX spectrum of specimens of particles for Al/10Al_2O_3/5Gr.

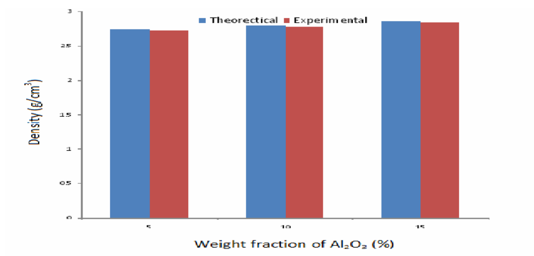

Fig. 5. Influence of Al_2O_3 particle on density.

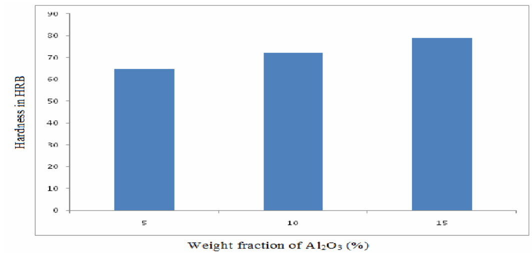

Fig. 6. Influence of Al_2O_3 particle on hardness.

increases with addition of Al_2O_3, which is mainly because of higher density of Al_2O_3 particle. The increase in density also indicates that the fabricated composites attain an improved bonding between the matrix and reinforcement [16]. From the Fig. 6, hardness increases with increase in Al_2O_3 content. This is because Al_2O_3 acts as a barrier to dislocation flow in aluminum matrix. Therefore, the increase of Al_2O_3 will give more barriers and hence low dislocation density, which increases the hardness of the composites [17].

3.3 Specific wear rate

The final regression equation developed using Design Expert 10 software for the specific wear rate is given below

$$\text{Specific wear rate} = +1.63042E\text{-}006 - 5.49613E\text{-}007 * s - 3.89015E\text{-}008 * f - 2.68830E\text{-}008 * w + 5.54531E\text{-}009 * s * f + 6.67250E\text{-}010 * f * w + 8.49512E\text{-}008 * s^2 + 2.03688E\text{-}010 * f^2. \quad (5)$$

The negative sign in the co-efficient indicates that response decreases as the parameter increases. From Eq. (5) it is clear that the specific wear rate decreases as the speed, load and weight fraction of Al_2O_3 increase. Similar findings were also

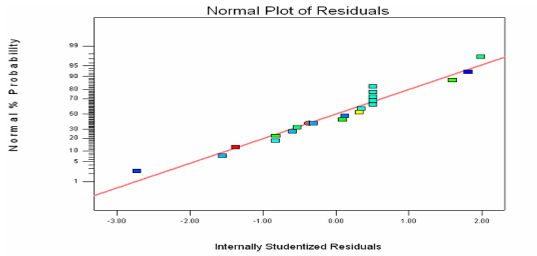

Fig. 7. Normal probability plot for residuals.

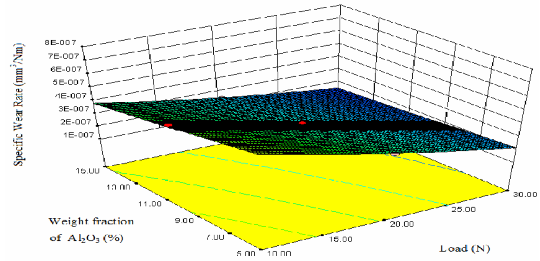

Fig. 8. 3D surface for specific wear rate of weight fraction of Al_2O_3 vs load.

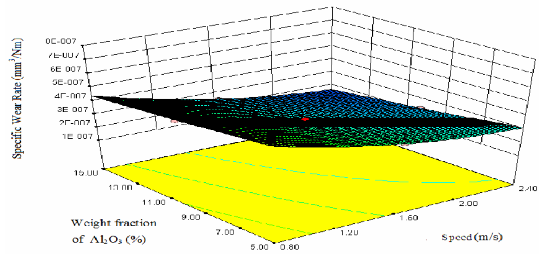

Fig. 9. 3D surface for specific wear rate of weight fraction of Al_2O_3 vs speed.

observed by Dharmalingam et al. [18]. From Table 4, the model value of 305.71 indicates the model is significant and the lack of Fit F-value of 6.60 implies the lack of fit is not significant for specific wear rate. There is only a 0.01% chance that a "Model F Value" this large could occur due to noise. The R^2 value lies between 0 and 1. A value close to 1 is desirable. The R^2 value is 0.99, which means that the model has good relationship between independent variables and response. From the ANOVA Table 4, it is clear that load is the most dominant factor that affects the specific wear rate of composites. Among the interaction load and speed contribute more than the other variables considered. Fig. 7 displays the normal probability plot of the residuals. From the Fig. 7 it is clear that errors are normally distributed as the residuals fall in a straight line.

The 3D interaction significant surface plots are shown in the Figs. 8 and 9, which depict that load and speed contribute more for specific wear rate than weight fraction. From the Fig. 8, as load increases the specific wear rate decreases. This is because the hard Al_2O_3 particles present in the composites increase the thermal stability of the matrix, which ultimately results in improved wear resistance at higher loads [18-21]. The decreasing nature with respect to load indicates the improved wear resistance performance at higher loads. Specific wear rate is high at low speed, whereas, as the specific wear rate decreases as the speed increases. Also, increase in speed decreases the specific wear rate for all range of parameters considered, indicating improved wear resistance at the higher velocities, as inferred from Fig. 9. This is attributed to the fact that at higher speed the interfacial temperatures are higher, which results in increasing oxidation of aluminum alloy, resulting in the formation of thick oxide film that exists between the sliding surfaces, protecting them from wear and thus lowering the wear rate [22]. From Figs. 8 and 9, it is suggested that specific wear rate decreases for all weight fraction of Al_2O_3. This is because Al_2O_3 protects the soft Al 6061 matrix, which results in decreased wear rate. As the Al_2O_3 increases, the hardness of the composites increases, resulting in better wear resistance. During sliding the soft matrix that surrounds the reinforcement is worn out soon. Therefore, the contact is only with the hard reinforcement particle and the counter body results in particle decoherence. The wear rate will be mostly controlled at particles decoherence. Thus the increase in Al_2O_3 particles decreases the specific wear rate.

3.4. Single response optimization

To set the specific wear rate to minimum, optimization of the process variables is required. The optimization is done by RSM-based desirability analysis. In the desirability-based approach, different best solutions are obtained. The solution with the highest desirability is preferred. The goal set and limits for optimization are shown in Table 5. Estimated contour plot for desirability is presented in Fig. 10. These response contours can help in the prediction of desirability at any zone of the experimental domain [23]. The three optimum solutions are shown in the Table 6: the improvement in the wear resistance of the composites became more prominent at high speed, high load and high weight fraction of Al_2O_3.

3.5 Verification of the optimal variables through confirmation test

The last step in design of experiment is the confirmation test, which is performed to check the validity of the optimization procedure. From the previously obtained optimized process variables, new experiments are conducted. The result obtained from the confirmation test is compared with the predicted value shown in the Table 7. From the Table 7, it is clearly understood the predicted results are close to the experiment's values. The error percentage observed in the Table 7 is due to vibration of the machine, environmental conditions, and the surface finish of both the pin and the disc [22]. Also, SEM image shown in Fig. 11 performed at the optimized condition shows fewer grooves and surface damages, which also confirms that the performed model can be used to evaluate the wear of hybrid composites.

Table 5. Goals set and limits for optimization.

Name	Goal	Lower limit	Upper limit	Lower weight	Upper weight	Impor-tance
Speed (m/s)	is in range	0.8	2.4	1	1	3
Load (N)	is in range	10	30	1	1	3
Wt of alu-mina (%)	is in range	5	15	1	1	3
Specific wear rate (mm^3/Nm)	minimize	1.15E-07	8.03E-07	1	1	3

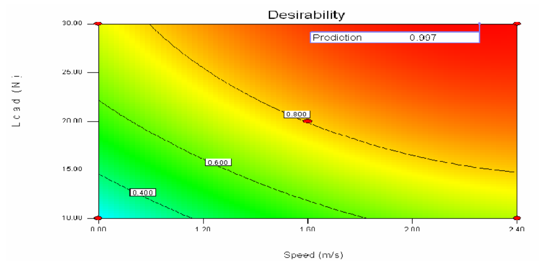

Fig. 10. Desirability chart.

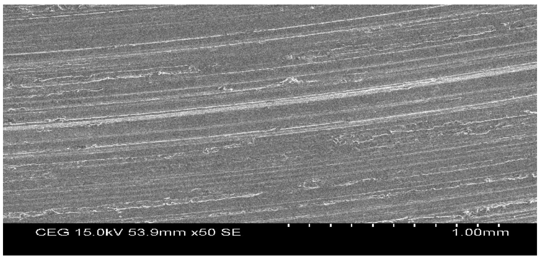

Fig. 11. SEM micrograph of $Al/Al_2O_3/Gr$ at s = 2.46 (m/s), f = 30 (N) and w = 15 (%).

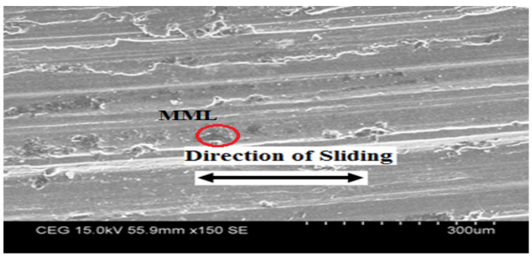

Fig. 12. SEM micrograph of $Al/Al_2O_3/Gr$ at load of 10 N.

3.6 Surface morphology

To investigate the wear mechanism in detail, the surfaces of the worn samples were examined under SEM. The SEM micrographs are in Figs. 12 and 13. Figs. 12 and 13 show grooves and particle pull out during sliding. At low load the grooves are very fine (Fig. 12) and they extend to scratches (Fig. 13) as the load increases. This is because, at higher loads the particle pulling out takes place and they act as an abrasive particle between the pin and the disc. These hard ceramic par-

Table 6. Optimal process variables for specific wear rate.

Sl. No	Speed (m/s)	Load (N)	Wt of alumina (%)	Specific wear rate (mm^3/Nm)	Desirability	
1	2.46	30	15	1.15787E-007	0.997	Selected
2	2.26	20.20	13.98	1.17673E-007	0.996	
3	2.20	20.20	14.28	1.18489E-007	0.995	

Table 7. Confirmation test.

Sl.No	Speed (m/s)	Load (N)	Wt of alumina (%)	Specific wear rate (mm^3/Nm)		
				Exp	Pred	Error %
1	2.46	30	15	1.15787E-007	1.1789E-007	1.8
2	2.26	20.50	13.98	1.17673E-007	1.216E-007	4.2

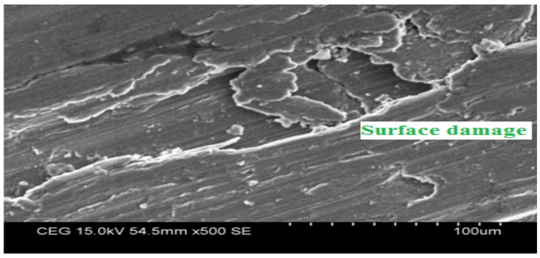

Fig. 13. SEM micrograph of $Al/Al_2O_3/Gr$ at load of 30 N.

ticles plough the surface of the soft Al 6061 forming an abrasive wear mechanism [24]. The addition of Gr particle plays a vital role in the wear mechanism. The graphite particle acts as solid lubricant during the sliding process. The graphite particles smear out of the matrix during sliding, forming a mechanical mixed layer which reduces the contact between the sliding surfaces [25]. This results in reduced metal to metal contact, which improves the wear resistance of Al $6061/Al_2O_3/Gr$ hybrid composites under different sliding conditions. Also Figs. 12 and 13 show surfaces cracks and wear scars running parallel to the sliding distance at higher loads. The worn pin surface shows white patches because of the formation of oxide wear throughout the surface. Therefore, it is concluded that abrasive wear is the dominant one followed by oxide wear.

4. Conclusions

The application of RSM and CCD was used for modeling and analyzing the influence of process variables on specific wear rate is presented. The article also addressed the optimization of process variables by RSM based desirability approach. The following conclusions are drawn:

- The microstructure of the composite exhibits uniform distribution of particles in the Al matrix.
- The density and hardness of the composites increase with increase in Al_2O_3 particles.

- The CCD is effectively used to optimize the sliding wear behavior of Al/Al_2O_3/Gr hybrid composites.
- From the ANOVA, it is inferred that load is the most dominant factor that affect specific wear rate followed by speed and weight fraction of Al_2O_3.
- From the desirability approach, high speed, high load and high weight fraction of Al_2O_3 result in optimum specific wear rate.
- From the SEM, the dominant wear mechanism is the abrasive wear caused by hard Al_2O_3 particle pull out.

Acknowledgment

The authors gratefully acknowledge the financial support of Sri Chandrasekharendra Saraswathi Viswa Mahavidyalaya kanchipuram, India for carrying out this research work. The authors wish to thank Assistant Professor Mrs. P. Bindhu English Department, SCSVMV University for reading and refining this manuscript.

Nomenclature

MMC : Metal matrix composites
SEM : Scanning electron microscope
Al_2O_3 : Alumina

References

[1] A. Arun Premnath, T. Alwarsamy and T. Rajmohan, Experimental investigation and optimization of process parameters in Milling of hybrid metal matrix composites, *Materials and Manufacturing Processes,* 27 (10) (2012) 1035-44.

[2] R. K. Bhushan, Sudhir Kumar and S. Das, Fabrication and characterization of 7075 Al alloy reinforced with SiC particulates, *Int. J. Adv. Manuf. Technol.,* 65 (2013) 611-624.

[3] S. Muthu Kumar and B. K. Dhindaw, Preparation and characterization of binder less Mg/Mg alloy infiltrated SiCp reinforced composites, *J. of Materials Engineering and Performance,* 16 (5) (2007) 527-532.

[4] K. G. Prashanth, S. Kumar, S. Scudino, B. S. Murty and J. Eckert, Fabrication and response of $Al_{70}Y_{16}Ni_{10}Co_4$ glass reinforced metal matrix composites, *Materials and Manufacturing Processes,* 26 (10) (2011) 1242-1247.

[5] G. Reddy, Chandrakanth, K. Rajkumar and S. Aravindan, Fabrication of copper-TiC-graphite hybrid metal matrix composites through microwave processing, *Int. J. Adv. Manuf. Technol.*, 48 (2010) 645-653.

[6] M. Wenlin and Jinjun Lu, Effect of sliding speed on surface modification and tribological behavior of copper-graphite composite, *Tribol. Lett.*, 41 (2011) 363-370.

[7] V. R. Rajeev, D. K. Dwivedi and S. C. Jain, A fractional factorial design study of reciprocating wear behavior of Al-Si-SiCp Composites at Lubricated Contacts, *J. of Materials Engineering and Performance*, 20 (2011) 368-376.

[8] N. Vijaya Sai, M. Komaraiah and A. V. Sita Rama Raju, Preparation and properties of sintered copper-tin composites containing copper coated or uncoated fly ash, *Materials and Manufacturing Processes,* 23 (7) (2008) 651-657.

[9] S. Akgun, S. Şahin and F. Ustel, Wear behavior of plasma-sprayed Al-12Si/SiC composite coatings under dry and water-lubricated sliding, *Materials and Manufacturing Processes,* 24 (7-8) (2009) 909-912.

[10] B.-C. Goo and M.-H. Kim, *Characteristics of A356/SiCp and A390/SiCp composites, J. of Mechanical Science and Technology,* 26 (7) (2012) 2097-2100.

[11] W. Park, C. Park, H. Kim and S. Huh, Microstructure and wear characteristics on Al alloy matrix composite reinforced with Ni perform, *J. of Mechanical Science and Technology,* 26 (6) (2012) 1741-1746.

[12] E. Liu, Y. Gao, J. Jia and Y. Bai, Friction and wear behaviors of Ni-based composites containing graphite/Ag_2MoO_4 Lubricants, *Tribol Lett.*, 50 (2013) 313-322.

[13] L. Ceschini, G. Minak and A. Morri, Tensile and fatigue properties of the AA6061/20 vol.% Al_2O_3p and AA7005/10 vol.% Al_2O_3p composites, *Composites Science and Technology*, 66 (2006) 333-342.

[14] D. C. Montgomery, *Design and analysis experiments*, 5^{th} edition, New York, Wiley, USA (2001).

[15] G. B. Veeresh Kumar, A. R. K. Swamy and Ramesha A, Studies on properties of as-cast Al6061-WC-Gr hybrid MMCs, *J. of Composite Materials,* 46 (17) (2011) 2111-2122.

[16] Y. Sahin, Preparation and some properties of SiC particle reinforced aluminium alloy, composites, *Materials and Design,* 24 (2003) 671-679.

[17] K. R. Ahmad, J. B. Shamsul, L. B. Hussain and Z. Arifin Ahmad, The Effect of reinforcement particle size on the microstructure and hardness of Al/(Al_2O_3) composite via PM route, *12th Scientific Conference and 13th Annual General Meeting of Electron Microscopy Society of Malaysia*, Langkawi (2003).

[18] S. Dharmalingam and R. Subramanian, Analysis of dry sliding friction and wear behavior of aluminium_Al_2O_3 composites using taguchi's techniques, *J. of Composite materials,* 44 (18) (2010) 2161-77.

[19] A. T. Alpas and J. Zhang, Effect of Sic particulate reinforcement on the dry sliding wear of aluminium-silicon alloys (A356), *Wear,* 155 (1992) 83-104.

[20] H. Unal, A. Mimaroglu, U. Kadıoglu and H. Ekiz, Sliding friction and wear behaviour of polytetrafluoroethylene and its composites under dry conditions, *Materials and Design,* 25 (2004) 239-245.

[21] Z.-Z. Zhang, Q.-J. Xue, W.-M. Liu and W.-C. Shen, Friction and wear properties of metal powder filled PTFE composites under oil lubricated conditions, *Wear,* 210 (1997) 151-156.

[22] S. Basavarajappa and G. Chandramohan, Dry sliding wear behavior of metal matrix composites: A statistical approach, *J. of Materials Engineering and Performance,*

15 (2006) 656-660.
[23] T. Rajmohan and Palanikumar, Optimization of machining parameters for surface roughness and burr height in drilling hybrid composites, *Materials and Manufacturing Processes,* 27 (3) (2012) 320-328.
[24] S. Mahdavi and F. Akhlaghi, Effect of the graphite content on the tribological behavior of Al/Gr and Al/30SiC/Gr composites processed by in situ powder metallurgy (IPM) method, *Tribol Lett.*, 44 (2011) 1-12.
[25] S. Basavarajappa, G. Chandramohan, K. Mukund, M. Ashwin and M. Prabhu, Dry sliding wear behavior of Al 2219/SiCp-Gr hybrid metal matrix composites, *J. of Materials Engineering and Performance,* 15 (2006) 668-674.

A. Arun Premnath graduated in Mechanical Engineering from University of Madras, India in 2003 and received his Masters in CAD from Anna University Chennai, India in 2006. He is currently an Assistant Professor in the Department of Mechanical Engineering in Sri Chandrasekharendra Saraswathi Viswa Maha Vidyalaya University Kanchipuram, India. His research is in machining of composites, fabrication and characterization of composites, wear behavior of composites and currently extending his knowledge by undergoing Ph.D. studies on composites materials.